Constrained Rouse model of rubber viscoelasticity

W. L. Vandoolaeghe and E. M. Terentjev[a)]
Cavendish Laboratory, Madingley Road, Cambridge CB3 0HE, United Kingdom

(Received 25 April 2005; accepted 23 May 2005; published online 22 July 2005)

In this work we use a new approach to investigate the equilibrium and linear dynamic-mechanical response of a polymer network. The classical Rouse model is extended to incorporate quenched constraints on its end-boundary conditions; a *microscopic* stress tensor for the network system is then derived in the affine deformation limit. To test the model we calculate the macroscopic stress in equilibrium, corresponding to the long-time limit of relaxation. Particular attention is paid to the treatment of compressibility and hydrostatic pressure in a sample with open boundaries. Although quite different in general, for small strains the model compares well with the classic equilibrium rubber-elasticity models. The dynamic shear modulus is obtained for a network relaxing after an instantaneous step strain by keeping track of relaxation of consecutive Rouse modes of constrained network strands. The results naturally cover the whole time range—from the dynamic glassy state down to the equilibrium incompressible rubber plateau. © *2005 American Institute of Physics*.

[DOI: 10.1063/1.1955445]

I. INTRODUCTION

For more than half a century theorists have tried to model the equilibrium and dynamical response of polymer networks. Modern understanding of network or *rubber* elasticity has come a long way since the first molecular models were developed in the 1930s.[1] Recent equilibrium theories are sophisticated and try to incorporate topological constraints from cross-links and entanglements, excluded volume effects, and network features such as dangling ends, inhomogeneities, and noninteracting strands.[2–4] Although generally successful and certainly valid conceptually, not one of these theories provides a completely adequate understanding of rubber elasticity. The predicted stress-strain forms and elastic moduli under various nontrivial types of deformation still show discrepancies with the experiment. Compared to the developed state of understanding of equilibrium (long-time) mechanical response, general dynamical response theories for polymer networks are markedly less successful. Once again, a large body of seminal literature exists in the area of dynamics of uncross-linked polymer chains (melts and solutions),[5–8] however, the corresponding consistent approach to the dynamics and relaxation of fully percolating random networks simply does not exist.

The dynamic response of networks is a research area with great practical importance. Problems related to this field are diverse, and include acoustics, vibration damping, impact resistance, crack propagation, and the toughening of biological tissues. The applications of dynamic response to deformations are found in various technologies from automobile tires to construction suspensions, to vibration dampers, and are thus of ardent industrial interest.[9] Fundamental theoretical research provides the basis for investigating and predicting the properties of these systems. An extension of the tube-model theory for rubbers, first proposed by Edwards,[10] was based on the reptation theory.[11,12] On the other hand, the first theoretical attempts to provide a consistent dynamic-mechanical theory of polymer *networks*, e.g., Ref. 13, have not advanced much. Few theories go beyond the phenomenological level to try and link macroscopic properties of the system with molecular structure. One of the first attempts to derive a statistical dynamics of networks by employing a viscosity coefficient, as in the Rouse model, never managed to explain the full set of dynamic properties.[14] Recently, work has been done on flexible polymer network dynamics based on the tube-model approach.[15] By analyzing the relaxation of strands between cross-link points the model successfully obtained the linear complex modulus of a highly entangled rubbery network, albeit in the low frequency range only.

The aim of the present work is to "start at the beginning." We construct a simple Rouse theory, on the level of older *ideal* unentangled chains, but nonetheless geared towards a dynamic-relaxation description of randomly cross-linked networks. This model naturally allows an analytical description of the relaxation of an affinely deformed ideal network over the whole time range. Although such an entropic theory alone is not wholly satisfactory (for example, to examine glassy dynamics in short-time limit), it remains a self-consistent and interesting model to work with. The merit of the present constrained dynamic Rouse model lies in that it is the first model naturally covering an equilibrium *and* dynamic-relaxation ranges of network response. One hopes incorporating the required level of complexity, i.e., accounting for chain excluded volume and entanglement constraints, should be an easier next step since these ideas and techniques are developed.

A. Classical phantom models

In the simplest, ideal case, the cross-links holding together a network of entropic springs are responsible for network elasticity. The two classic models of rubber elasticity

[a)]Electronic mail: emt1000@cam.ac.uk

commonly referred to in the literature are the Kuhn (or affine) and the James-Guth (or phantom) models.[1,16] Both of these models are *phantom* in the sense that the excluded volume is ignored and chains may freely intersect. Another key idea is that the network strand conformations are assumed to be independent of one another, thus ignoring the long-range multichain correlations. The Kuhn model assumes an *affine* deformation: if a macroscopic rubber sample is deformed by the strain tensor $\mathbf{E}$, then the end-to-end (span) vector $\mathbf{R}$ of any subchain between two junction points will be equal to $\mathbf{E}\cdot\mathbf{R}$ after deformation. The affinity assumption implies that the cross-links are spatially fixed, and do not fluctuate. In the James-Guth model cross-links are essentially unrestricted in their own fluctuation, but the resultant free energy

$$\mathcal{F}(\boldsymbol{\lambda}) = \frac{1}{2}N_c k_B T \,\mathrm{Tr}[\mathbf{E}^{\mathsf{T}}\cdot\mathbf{E}] = \frac{1}{2}N_c k_B T\left(\lambda^2+\frac{2}{\lambda}\right) \quad (\text{if } \lambda_z=\lambda, \lambda_{x,y}=\lambda^{-1/2}), \tag{1}$$

is only altered by a factor of $\frac{1}{2}$. Here k_BT is the Boltzmann temperature and N_c is the number of cross-links in the network sample. The last line of Eq. (1) is for a uniaxial stretch by a factor λ and uses an explicit constraint of material incompressibility, which will be a subject of special discussion in Sec. IV B below. The force required to the change the length of the sample from L_{z_i} to L_{z_f} is equal to the change in the deformation free energy $\mathcal{F}(\boldsymbol{\lambda})$ with respect to the change in the sample size along the axis of deformation

$$f_z = \frac{\partial\mathcal{F}}{\partial L_z} = \frac{\partial\mathcal{F}}{\partial(\lambda L_{z_i})} = \frac{N_c k_B T}{L_{z_i}}\left(\lambda-\frac{1}{\lambda^2}\right). \tag{2}$$

The *true* stress $\sigma_{\alpha\beta}$ in an elastic medium is the ratio between the force applied in the α direction and the cross-sectional area of the strained sample perpendicular to the β axis. For the current example of uniaxial deformation the true stress is

$$\sigma_{zz} = \frac{f_z}{L_{x_f}L_{y_f}} = \frac{\lambda}{V_i}\frac{\partial\mathcal{F}}{\partial\lambda} = \tilde{c}k_B T\left(\lambda^2-\frac{1}{\lambda}\right), \tag{3}$$

where $\tilde{c}=N_c/V_i$ is the average cross-link density of the network sample. A more convenient stress to measure in experiments is the so-called *engineering* or nominal stress defined as the force applied, divided by the *original* cross-sectional area of the reference sample conformation:

$$\sigma_{zz(\mathrm{eng})} = \frac{f_z}{L_{x_i}L_{y_i}} = \tilde{c}k_B T\left(\lambda-\frac{1}{\lambda^2}\right). \tag{4}$$

A recent network model by Panyukov and Rabin,[17] based on the Deam and Edwards model of instantaneous cross-linking of ideal chains,[18] led to a similar stress-strain relationship as in Eq. (3), but with a different numerical front factor. They calculated a mean-field free energy by means of an elegant field-theoretic method involving a double limiting procedure: the replica trick and a generalization of the De Gennes $n=0$ method.[19]

In this paper we use a microscopic stress-tensor method, which, albeit less advanced for modeling rubber elasticity than the above, can more naturally be extended to the dynamical problems of cross-linked polymers.

B. Assumptions and outline

Apart from the assumption about the chains ideality (neglecting both internal energy contributions and the topology, which is the customary first approximation), we also assume that our model system is a homogeneous material where local clustering of cross-links is negligible. In reality, the links build up in time and one cross-link will affect the neighboring chain density, therefore influencing the position of the next link, and clusters of junctions may appear.[17,20,21] As the cross-link density is increased there is an abrupt change of the melt from a viscous liquid to a solid, elastic gel that shows no tendency to flow. At this so-called *gel point* a giant cluster or network spans the whole sample. The theoretical explanations for how the transition actually takes place still remain a worthwhile pursuit.[22,23] In this paper, we calculate the stress for a network system well above any gel-point threshold.

This article is organized as follows. After briefly reviewing the fundamental starting points, we next turn to the case of constrained Rouse model in Sec. II. Although the principles of Rouse dynamics are a truly classical foundation of polymer physics, the formalism for a chain with constrained end points required new development. This permits an adaptation of the microscopic stress tensor to the case of a cross-linked polymer network, which is the subject of Sec. III. The resulting expression for the dynamic-elastic stress tensor forms the backbone of the remaining work. Section IV deals with the long-time limit of the general theory, when the deformed network is at, or near the equilibrium. This leads us to another theory of rubber elasticity. Although we do not focus on this aspect, aiming to develop the dynamic theory, the long-time limit of current model is compared with the "standard" experimental data of rubber deformations, as well as with classic rubber elasticity models. In deriving the true stress for the strained network system, it is vital to treat volume relaxation and appropriate boundary constraints—phenomena largely ignored in many other theories and not well represented in the literature. Section IV B deals with the key aspects of (in)compressibility. The equilibrium calculation provides the basic groundwork for understanding and approaching the actual problem of studying dynamics. In Sec. V we approach the full linear dynamic response, that is, how a rubbery network relaxes with time after a sudden deformation is applied. Here, again, we pay attention to the aspects of dynamic volume relaxation and derive the time-dependent linear-response moduli and the Poisson coefficient. In all of this work we assume that all deformations are homogeneous, that is, the stress and strain components do not vary with position in the body. Lastly, we conclude and give an outline of possible improvements and future developments.

II. CONSTRAINED ROUSE DYNAMICS

Here we consider the dynamics of an individual ideal chain. The starting point for describing the motion of the polymer is the Rouse model of beads, each connected to its nearest neighbor with Gaussian springs.[5] When a polymer liquid is sheared, every segment of the polymer chain will experience a certain friction together with random forces, balancing the input energy of thermal fluctuations and the dissipation. In the Rouse model this effect is modeled as a continuous viscous background for each given segment. In dense polymeric melts, in contrast with normal liquids or dilute polymeric solutions, this first-order approach is acceptable.

For a Rouse system at a given temperature T, the intramolecular forces are regarded as simple harmonic with spring constant $k=3k_BT/\ell^2$, with ℓ the segment size, and $\mathcal{U}=\frac{1}{2}k\Sigma(\mathbf{r}_n-\mathbf{r}_{n-1})^2$ the potential energy of each segment. If ζ is the friction coefficient of a monomer and $\mathbf{f}_n$ the stochastic force (white thermal noise), the position of the monomers (chain segments) satisfies a Langevin equation, $\zeta\, d\mathbf{r}_n/dt=-\partial U/\partial\mathbf{r}_n+\mathbf{f}_n$. In the overdamped limit the frictional force felt by monomer n is balanced by the random force $\mathbf{f}_n$, as well as the sum of the forces acting on it from its two neighbors, $k(\mathbf{r}_{n-1}-\mathbf{r}_n)$ and $k(\mathbf{r}_{n+1}-\mathbf{r}_n)$. If $\mathbf{r}_n$ denotes the position of the nth monomer, the continuum limit of this Langevin equation can be written as

$$\zeta\frac{d\mathbf{r}_n}{dt}=k\frac{\partial^2\mathbf{r}_n}{\partial n^2}+\mathbf{f}_n. \tag{5}$$

Since the interactions between the different monomer segments (or *beads*) are localized to nearest neighbors, each of the N segments $\mathbf{r}_n$ satisfies a linear differential equation decoupled from the the other beads. The dynamics of the whole chain can thus be described by a set of normal modes. For a *free* chain the elastic force vanishes at the ends, which implies the following boundary conditions:

$$\left.\frac{\partial\mathbf{r}_n}{\partial n}\right|_{n=0}=0 \quad \text{and} \quad \left.\frac{\partial\mathbf{r}_n}{\partial n}\right|_{n=N}=0. \tag{6}$$

In this case the amplitudes of the normal modes $\mathbf{x}_p$ are defined as $\mathbf{x}_p(t)\equiv 1/N\int_0^N dn\,\cos(p\pi n/N)\mathbf{r}_n(t)$, where p is an integer denoting the pth mode.[5] This formalism leads to the classical Rouse model, described in every book on polymer physics.

However, in a network the chain ends are cross-linked and thus constrained to a certain extent. As a start, let us consider the ends to be completely fixed, i.e.,

$$\mathbf{r}|_{n=0}=0 \quad \text{and} \quad \mathbf{r}|_{n=N}=\mathbf{R}. \tag{7}$$

To accommodate these new boundary conditions, we have to decompose the harmonic-oscillator motion of Eq. (5) into the normal modes $\{\mathbf{x}_p\}$, which are slightly different from the classical free-ends Rouse form

$$\mathbf{x}_p(t)\equiv\frac{1}{N}\int_0^N dn\;\mathbf{r}_n(t)\sin\left[\frac{(p-1/2)\pi n}{N}\right], \tag{8a}$$

$$\mathbf{r}_n(t)=2\sum_{p=1}^{\infty}\mathbf{x}_p(t)\sin\left[\frac{(p-1/2)\pi n}{N}\right]. \tag{8b}$$

Then the Langevin equation (5) with the associated stochastic force transforms to a set of decoupled Rouse equations,

$$\zeta_R\frac{d\mathbf{x}_p}{dt}=-k_p\mathbf{x}_p+\hat{\mathbf{f}}_p, \tag{9}$$

with $\langle\hat{f}_{p\alpha}(t)\hat{f}_{q\beta}(t')\rangle=2\zeta_Rk_BT\delta_{pq}\delta_{\alpha\beta}\delta(t-t')$ (where $\zeta_R\equiv 2N\zeta$) and the initial conditions $\mathbf{x}_p(0)$. As usual, this is a diffusion problem for an effective "particle" in a harmonic potential with a constant

$$k_p=\frac{2\pi k(p-1/2)^2}{N}=\frac{6\pi^2k_BT}{Nb^2}\left(p-\frac{1}{2}\right)^2. \tag{10}$$

From Eq. (8b) the end-to-end vector $\mathbf{R}(t)\equiv\mathbf{r}_N(t)-\mathbf{r}_0(t)$ for the constrained Rouse description can be written as

$$\mathbf{R}(t)=-2\sum_{p=1}^{\infty}(-1)^p\mathbf{x}_p(t), \tag{11}$$

in terms of the normal coordinates, again with a subtle difference with respect to the classical Rouse problem.

In this section, and in this work, we focus on a Rouse chain with fixed end points. There are, perhaps, surprisingly, only few examples in the literature when Rouse modes have been derived for other boundary conditions: for ends fixed at the same point (a loop with $\mathbf{r}_n=\mathbf{r}_0=\mathbf{0}$),[24] for one end fixed and one free (a tethered chain),[25,26] and for a block copolymer system with free ends, but chain connectivity at the interblock junction.[27]

III. A NETWORK OF ROUSE CHAINS

Section II introduced the main ingredients for studying phantom network dynamics, but is so far only applicable to a single, constrained chain. Now consider a random network of such end-linked chains, deformed by strain tensor $\mathbf{E}$, and let each strand $\mathbf{R}_0$ (between two connected junction points) be deformed affinely, that is, $\mathbf{R}=\mathbf{E}\cdot\mathbf{R}_0$. We assume that the network is initially isotropic. Cross-links are permanent and will impose the topological constraints on the chains, given that the cross-link density is high enough. Since the cross-links are randomly quenched, fixing the N and the initial $\mathbf{R}_0$ for each strand, the probability to find a corresponding deformed strand is given by the same distribution function $\mathbb{P}(\mathbf{R}_0)$, as has been established at network formation. The notation $[\cdots]_{\mathbb{P}}$ refers to the quenched average over the simplest appropriate probability distribution

$$\mathbb{P}(\mathbf{R}_0)=\left(\frac{3}{2\pi N\ell^2}\right)^{3/2}\exp\left(-\frac{3\mathbf{R}_0^2}{2N\ell^2}\right). \tag{12}$$

Furthermore, since $\mathbf{x}_p(t)$ depends linearly on the stochastic force $\hat{\mathbf{f}}_p(t)$, which is the annealed variable, the ensemble average $\langle\cdots\rangle_\psi$ is naturally replaced by the time average calculated over the functional distribution $\psi[\hat{\mathbf{f}}_p(t)]$. Therefore, the notation $\langle\cdots\rangle_\psi$ denotes the time-average of the components of stochastic force $\hat{\mathbf{f}}_p(t)$ over the distribution

$$\psi[\hat{f}_{p\alpha}(t)] \propto \exp\left(-\frac{1}{4\zeta_R k_B T}\int dt \hat{f}_{p\alpha}(t)^2\right). \tag{13}$$

The microscopic stress tensor $\sigma_{\alpha\beta}$ of a viscoelastic material consists of the stress contribution due to the polymers $\sigma^{(p)}_{\alpha\beta}$, the solvent molecules $\sigma^{(s)}_{\alpha\beta}$, and an isotropic pressure term $\sim k_B T\delta_{\alpha\beta}$, as follows:

$$\sigma_{\alpha\beta} = \underbrace{\frac{c}{N}\sum_{n=1}^{N}\left\langle \frac{\partial \mathcal{U}}{\partial r_{n\alpha}} r_{n\beta}\right\rangle_{\psi}}_{\sigma^{(p)}_{\alpha\beta}} + \sigma^{(s)}_{\alpha\beta} + \langle P\rangle\delta_{\alpha\beta}. \tag{14}$$

The last two contributions are of minor significance for a phantom network model and are thus neglected from here onwards. In the above c is the monomer density, N is the number of segments of a given polymer chain, so that $c/N = \tilde{c}$ is the number of chains per unit volume in the system. These monomers (or beads) have position vectors $\mathbf{r}_n(t)$ and find themselves subjected to a potential $\mathcal{U}$. For the Rouse model of constrained chains the stress tensor Eq. (14), in the continuous limit, is given by

$$\sigma^{(p)}_{\alpha\beta} = \frac{c}{N}k\int_0^N dn\left\langle \frac{\partial r_{n\alpha}}{\partial n}\frac{\partial r_{n\beta}}{\partial n}\right\rangle_{\psi} \tag{15}$$

$$= \frac{c}{N}\sum_p k_p \langle x_{p\alpha}(t)x_{p\beta}(t)\rangle_{\psi}. \tag{16}$$

The stress tensor of the whole network can be expressed as the ensemble average of $\sigma_{\alpha\beta}$ over the quenched probability to find the given strand, which is the Eq. (12). This operation is denoted by the square brackets in Eq. (17) below. Crucially, we must implement the constraint ensuring that only the end-to-end vectors deform affinely, leading to

$$\sigma_{\text{netw},\alpha\beta} = \frac{\tilde{c}}{\mathcal{V}}\sum_{p=1}^{\infty} k_p\left[\left\langle x_{p\alpha}(t)x_{p\beta}(t)\,\delta\left(\mathbf{E}\cdot\mathbf{R}_0 + 2\sum_{q=1}^{\infty}(-1)^q\mathbf{x}_q(t)\right)\right\rangle_{\psi}\right]_{\mathbf{P}(\mathbf{R}_0)}, \tag{17}$$

where $\mathcal{V}$ is a normalization factor of the ensemble averaging. $\mathcal{V}$ has the dimensions of inverse volume. The need for the constant $\mathcal{V}$ arises naturally since the Dirac-delta constraint has dimensionality of inverse volume; this constant turns out to be equal to $\mathcal{V}=(3/2\pi N\ell^2)^{3/2}$. After exponentiating the δ constraint as

$$\frac{\mathcal{V}}{(2\pi)^3}\int_{-\infty}^{\infty} d\boldsymbol{\phi} e^{i\boldsymbol{\phi}\cdot\left(\mathbf{E}\cdot\mathbf{R}_0 + 2\sum_{q=1}^{\infty}(-1)^q\mathbf{x}_q(t)\right)}, \tag{18}$$

and performing the Gaussian integration over $\mathbf{R}_0$, with probability distribution in Eq. (12), and then another over the auxiliary vector field $\boldsymbol{\phi}$, the stress tensor becomes

$$\sigma_{\text{netw},\alpha\beta} = \frac{\tilde{c}}{[\det \mathbf{E}\mathbf{E}^{\mathsf{T}}]^{1/2}}\sum_{p=1}^{\infty} k_p\left\langle x_{p\alpha}(t)x_{p\beta}(t)\exp\left\{-\frac{6}{N\ell^2}\sum_{q,r}^{\infty}\sum_{\gamma,\nu=1}^{3}(-1)^{q+r}x_{q\gamma}(t)(\mathbf{E}\mathbf{E}^{\mathsf{T}})^{-1}_{\gamma\nu}x_{r\nu}(t)\right\}\right\rangle_{\psi}, \tag{19}$$

which still depends on the solution $x_{p\alpha}(t)$ of the Langevin equation (9), the specific type of deformation $\mathbf{E}$, and another functional integration over the remaining set of chain stochastic variables $\{\mathbf{x}_p(t)\}$. Recall that there are other contributions to $\sigma_{\alpha\beta}$, in Eq. (14), apart from the polymeric part we are considering now. However, in our model for a network we assume the polymer concentration to be sufficiently high such that the viscous stress (from intermolecular collisions) is negligibly small compared with the elastic stress due to *intramolecular* forces. The issue with hydrostatic pressure is quite delicate in an elastic system; we devote the whole Sec. IV B to this problem of volume relaxation and effective (in)compressibility.

In order to compute the continuum elastic stress tensor (19) one must know the solution for $\mathbf{x}_p(t)$ in terms of stochastic force and the initial conditions. Before embarking on the general solution of this problem, we first examine the limit of long times. Although our ultimate purpose is to describe the full dynamical range of relaxations, testing the model against equilibrium rubber elasticity is an important reference point.

IV. PRACTICAL IMPLICATION I: EQUILIBRIUM RESPONSE

First we shall implement the formalism developed in Sec. III for a network system that has reached its equilibrium state. At $t\to\infty$, when the memory of the initial condition for the Langevin equation is lost, the stochastic solution of Eq. (9) is given by

$$x_{p\alpha}(t) = \frac{1}{\zeta_R}\int_{-\infty}^{t} e^{-(t-t')/\tau_p}\hat{f}_{p\alpha}(t')dt', \tag{20}$$

where $\tau_p \equiv \zeta_R/k_p$ is the mode relaxation time. This defines the famous Rouse time, the longest time of relaxation of the lowest ($p=1$) collective mode of a chain N segments long: $\tau_R = \zeta N^2 \ell^2/(3\pi^2 k_B T)$. In order to complete the averaging with respect to the distribution function $\psi[f_{p\alpha}(t)]$, we substitute the equilibrium solution Eq. (20) for $\mathbf{x}_p(t)$, to obtain an expression for the stress tensor in Eq. (19) in the limit of $t \gg \tau_R$,

$$\sigma_{\mathrm{netw},\alpha\beta} = \frac{\tilde{c}}{\zeta_R^2}[\det \mathbf{E}\mathbf{E}^{\mathsf{T}}]^{-1/2} \sum_{p=1}^{\infty} k_p \int_{-\infty}^{t} dx \int_{-\infty}^{t} dy\, e^{-(2t-x-y)/\tau_p} \int [\mathcal{D}f] f_{p\alpha}(x) f_{p\beta}(y) \times \exp\left\{ -\frac{1}{2} \sum_{\gamma,\nu=1}^{3} \sum_{q,r=1}^{\infty} \int_{-\infty}^{\infty} dt' \int_{-\infty}^{\infty} dt'' f_{q\gamma}(t') \mathbf{M}_{q,r}^{\gamma,\nu}(t',t'') f_{r\nu}(t'') \right\}. \tag{21}$$

Introducing the tensor notation $\mathbf{M}$ enables us to write the stress $\sigma_{\mathrm{netw},\alpha\beta}$ as a compact Gaussian path integral. It consists of two parts: a *diagonal* contribution due to the distribution function $\psi[f_{p\alpha}(t)]$, and the additional part coming from the exponent in Eq. (19). The latter part is only integrated and defined for times $\leqslant t$. This upper limit on time is dealt with by using Heaviside (step) functions. The tensor $\mathbf{M}$ can thus be written as

$$\mathbf{M}_{qr}^{\gamma\nu}(t',t'') = A\,\delta(t'-t'')\,\delta_{qr}\delta_{\gamma\nu} + (-1)^{q+r} b (\mathbf{E}\mathbf{E}^{\mathsf{T}})_{\gamma\nu}^{-1} e^{-(t-t')/\tau_q} e^{-(t-t'')/\tau_r} \Theta(t-t')\Theta(t-t'') \equiv A\mathbf{I} + b\mathbf{B}. \tag{22}$$

We use shorthand for the combinations of material parameters: $A=(2\zeta_R k_B T)^{-1}$ and $b=12/(\zeta_R^2 N \ell^2)$. The matrix $\mathbf{B}$ depends on the times and the applied strain tensor: $\mathbf{B} = (-1)^{q+r}(\mathbf{E}\mathbf{E}^{\mathsf{T}})_{\gamma\nu}^{-1} e^{-(t-t')/\tau_q} e^{-(t-t'')/\tau_r}$. In order to compute the stress tensor given by the Gaussian integral in Eq. (21) we have to find the determinant of $\mathbf{M}_{qr}^{\gamma\nu}(t',t'')$ as well as the correct inverse matrix element. The full calculation is presented in the Appendix, and here we shall only quote the results. If no assumption is made about the type of deformation, then from Eqs. (A3), (A6), (A7), and (21), the general expression for the equilibrium stress tensor at $t \to \infty$ is given by

$$\sigma_{\mathrm{netw},\alpha\beta} = \frac{\tilde{c} k_B T}{[\mathrm{Det}\, \mathbf{E}\mathbf{E}^{\mathsf{T}}]^{1/2}} (1 + [\mathbf{E}\mathbf{E}^{\mathsf{T}}]_{\alpha\beta}^{-1})^{-1} \times \exp\left[-\frac{1}{2} \sum_n \frac{(-1)^{n+1}}{n} \mathrm{Tr}\{(\mathbf{E}\mathbf{E}^{\mathsf{T}})^{-n}\} \right]. \tag{23}$$

The value of the trace and the result of summation in the exponent depend on the type of deformation $\mathbf{E}$ and we shall next investigate two specific cases.

A. The stress tensor: Diagonal deformations

If $\mathbf{E}$ is a diagonal deformation, say, uniaxial or biaxial extension then

$$\mathbf{E} = \begin{pmatrix} \lambda_1 & 0 & 0 \\ 0 & \lambda_2 & 0 \\ 0 & 0 & \lambda_3 \end{pmatrix} \Rightarrow \mathrm{Tr}\{(\mathbf{E}\mathbf{E}^{\mathsf{T}})^{-n}\} = \sum_\gamma E_{\gamma\gamma}^{-2n}. \tag{24}$$

In this case the stress tensor is given by

$$\sigma_{\alpha\beta} = \frac{\tilde{c} k_B T}{\prod_\gamma E_{\gamma\gamma}} (\delta_{\alpha\beta} + E_{\alpha\beta}^{-2})^{-1} \left[\prod_\gamma (1 + E_{\gamma\gamma}^{-2}) \right]^{-1/2} = 0 \quad \text{if } \alpha \neq \beta. \tag{25}$$

For an isovolumetric, uniaxial extension, or compression (see Fig. 1), $\lambda_1=\lambda_2=\lambda^{-1/2}$ from symmetry, and $\lambda_3=\lambda$, the stress σ_{uni} depends only on the single Cartesian extension ratio λ, as follows:

$$\sigma_{yy}^{\mathrm{uni},xx} = \tilde{c} k_B T (1+\lambda)^{-2} \left(1 + \frac{1}{\lambda^2} \right)^{-1/2}, \tag{26a}$$

$$\sigma_{\mathrm{uni},zz} = \tilde{c} k_B T (1+\lambda)^{-1} \left(1 + \frac{1}{\lambda^2} \right)^{-3/2}. \tag{26b}$$

In this type of extension the side surfaces are stress-free and one would therefore expect the corresponding principal stresses in to be zero. Why we are not finding this in Eq. (26a)? Most rubber-elasticity theories calculate the *change* in free energy upon deforming the network sample. Before determining the expressions for the stress, any indeterminate pressure terms are by that stage already subtracted or are simply discarded since they do not depend on the deformation λ. For this reason seminal literature always mentions that it is important to examine *relative* stress expressions only, cf. Ref. 28. It is known that these arbitrary pressure terms are due to a change in the volume of the network system during deformation. However, one cannot accept that hydrostatic pressure is different in an open sample of rubber with stress-free boundaries. We have to look more carefully at the effect of volume relaxation on these stress expressions. Since the present model works with the stress tensor from the onset—in contrast with a partition function and associated free energy, like most models—it is important to deal with this phenomenon correctly.

B. (In)compressibility and volume relaxation

Consider an initial polymer melt sample of volume V_0. After sufficient cross-linking a network is formed, contained in a volume V, smaller than the initial volume. This volume change, or syneresis, is caused by the reduction in overall entropy due to cross-linking, and is penalized by a bulk energy contribution $\frac{1}{2}\tilde{K}(\mathrm{Det}\,\mathbf{E}-1)^2$ in the elastic free-energy density, and correspondingly in stress by the amount $\tilde{K}(\mathrm{Det}\,\mathbf{E}-1)$. Here $\tilde{K}$ is a very large bulk modulus usually of the order 10^9 J/m^3 or greater.[29]

Our first task is to determine what the impact of syneresis is on the stress-tensor expression. Denote by $\mathbf{E}_0$ the ininitial deformation associated with volume relaxation after network formation. Since we expect this deformation to be small relative to any future imposed strain, as well as being isotropic, we have $\mathbf{E}_0=(1+a_0)\mathbf{I}$. For simplicity, we consider first the case of no additional external deformation. Then the stress tensor in Eq. (25) is only a function of a_0,

$$\sigma_{\mathrm{syn},\alpha\beta}=\frac{\tilde{c}k_\mathrm{B}T}{(1+a_0)^3}\delta_{\alpha\beta}(1+(1+a_0)^{-2})^{-1}\times(1+(1+a_0)^{-2})^{-3/2}+\tilde{K}[(1+a_0)^{-3}-1]\delta_{\alpha\beta}. \quad (27)$$

After network formation, the system will reach its equilibrium state, which implies that all the resultant stresses should be zero. Since the correction a_0 is expected to be small, we can expand Eq. (27) up to linear order in a_0 and solve for $\sigma_{\mathrm{syn},\alpha\beta}=0$. This step is equivalent to minimizing the free-energy density of the system as discussed in Ref. 29. The equilibrium solution for this syneresis correction is found to be

$$a_0^*=\frac{2\sqrt{2}\tilde{c}k_\mathrm{B}T}{-48\tilde{K}+\sqrt{2}\tilde{c}k_\mathrm{B}T}\propto-\frac{\tilde{c}k_\mathrm{B}T}{\tilde{K}}\ll 1. \quad (28)$$

Next, imagine imposing an external deformation $\mathbf{E}$, for example, the uniaxial extension. During this deformation a second volume relaxation is possible and should also be accounted for. The total deformation therefore takes the form $\mathbf{E}_{\mathrm{tot}}=\mathbf{E}_{\mathrm{uni}}(1+a)(1+a_0^*)$, where $\mathbf{E}_{\mathrm{uni}}$ is the strictly isovolumetric strain tensor and a_0^* is given by Eq. (28). When the sample is strained by $\mathbf{E}_{\mathrm{uni}}$, it will lead to the well-known rubber-elastic response, but *also* to an additional small bulk compression, represented by a, which is dependent on the imposed strain λ. Again, the underlying physical reason for this extra compression is the further reduction in conformational entropy on deformation. Substituting the total deformation into the stress tensor in Eq. (25), we have for the nonzero diagonal components,

$$\sigma_{\alpha\alpha}=\frac{\tilde{c}k_\mathrm{B}T}{(1+a_0^*)^3(1+a)^3}\left(1+\frac{E_{\alpha\alpha}^{-2}}{(1+a_0^*)(1+a)}\right)^{-1}\times\prod_{\eta=1}^{3}\left(1+\frac{E_{\eta\eta}^{-2}}{(1+a_0^*)^2(1+a)^2}\right)^{-1/2}+\tilde{K}[(1+a_0^*)^{-3}(1+a)^{-3}-1]. \quad (29)$$

The required second volume-relaxation correction a is uncovered by demanding that for, e.g., uniaxial extension in the $\hat{z}$ direction we should have $\sigma_{\mathrm{uni},xx}=\sigma_{\mathrm{uni},yy}=0$. Again, by expanding the stresses up to first order in a, one obtains a^* for which only $\sigma_{\mathrm{uni},zz}$ is nonzero. To present it explicitly, we must specify the axes and the principal imposed strain λ,

$$a^*\approx\frac{\tilde{c}k_\mathrm{B}T}{24K}\left((1+\lambda)(1+\lambda^2)^2\left(-8+\sqrt{2+\frac{2}{\lambda^2}}(1+\lambda)^2\right)\times(1+\lambda+\lambda^2+\lambda^3)\right)\left[\sqrt{1+\frac{1}{\lambda^2}}(1+\lambda)^4(1+\lambda^2)^3\right]^{-1}.$$

This volume-relaxation factor is written in the leading approximation in the small parameter, the ratio of shear to bulk modulus, simply to give the reader an idea of the expression structure. Only the exact, nonsimplified expression would achieve, on substitution into Eq. (29), the zero-stress conditions on free surfaces.

Lastly, after substituting a^* to Eq. (26b), we can now take the limit $\tilde{K}\to\infty$ and obtain the correct expressions for the stress in uniaxial deformation,

$$\sigma_{\mathrm{uni},zz}=\frac{\tilde{c}k_\mathrm{B}T(\lambda^3-1)}{(1+\lambda)^2(1+\lambda^2)(1+\lambda^{-2})^{1/2}},\qquad \sigma_{\mathrm{uni},xx}=\sigma_{\mathrm{uni},yy}=0. \quad (30)$$

The stress σ_{zz} vanishes when there is no deformation, that is, when $\lambda=1$. This behavior is expected, but is only obtained here *after* accounting for the bulk modulus term and by including small corrections to the overall strain tensor $\mathbf{E}$ due to volume relaxations. There are alternative approaches used in continuum mechanics of large deformations, e.g., Refs. 30 and 31, based on keeping the rigid constraint of $\mathrm{Det}\,\mathbf{E}=1$ by means of a Lagrange multiplier which has the meaning of system pressure (so that the actual stress is $\sigma_{\alpha\beta}-P\delta_{\alpha\beta}$). There are, however, many negative consequences of independently defining the hydrostatic pressure in a solid system with open boundaries.

The majority of mechanical tests on polymer networks are conducted in uniaxial extension. Together with the data from compression of the sample, it can portray interesting properties of the material. Figure 2 shows the predictions of the present model in Eq. (30). It is clear that this equilibrium model is far from being successful in predicting the observed

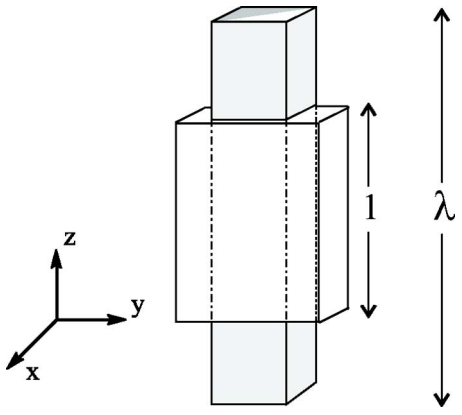

FIG. 1. A uniaxial extension, $\lambda_1=\lambda_2=\lambda^{-1/2}$, and $\lambda_3=\lambda$.

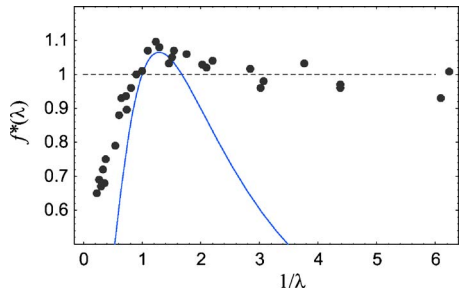

FIG. 2. The Mooney-Rivlin plot of reduced stress function $f^*=\sigma_{\mathrm{eng}}/G(\lambda-1/\lambda^2)$ vs. $1/\lambda$, together with a set of experimental uniaxial deformation data from Ref. 32, shown as dots. The phantom affine model is shown as the dashed line $f^*=1$, for comparison.

nonlinear response (although it does have the right qualitative features). One should not be surprised by that, as the present model ignores such key effects as chain entanglements. We remind the reader that our aim is to develop a basic framework for a consistent model of the dynamic response and in doing so we remain within the phantom chain approximation.

C. The stress tensor: Small deformation

Next we investigate Eq. (23) when $\mathbf{E}$ is a small deformation. Although the results in equilibrium regime are nearly trivial, this is the important limit as the reference point for the subsequent linear dynamic-mechanical theory. The strain tensor is $\mathbf{E}=\mathbf{I}+\mathbf{e}$, so that

$$\mathbf{E}\mathbf{E}^{\mathsf{T}}=\mathbf{I}+\mathbf{e}+\mathbf{e}^{\mathsf{T}}+\cdots\approx\mathbf{I}+2\boldsymbol{\varepsilon}. \tag{31}$$

In the last step we identified the symmetric part $\boldsymbol{\varepsilon}=\frac{1}{2}(\mathbf{e}+\mathbf{e}^{\mathsf{T}})$ of the general, infinitesimal strain tensor $\mathbf{e}$, and discarded insignificantly small terms of $\mathcal{O}(\boldsymbol{\varepsilon}^2)$.[33] For a small, simple shear $\mathrm{Tr}\,\boldsymbol{\varepsilon}=0$ and the determinant is given by $(\mathrm{Det}\,\mathbf{M})^{-1/2}\simeq e^{-1/2\ \mathrm{Tr}\ln A\mathbf{I}}/2\sqrt{2}$. The resulting stress again gives nonzero components that ought not to exist, for example, $\sigma_{xx}\simeq(\tilde{c}k_{\mathrm{B}}T)/4\sqrt{2}$. When we take syneresis into account by including a bulk modulus term and the a_0^* correction in Eq. (28), as was done in Sec. IV B, the diagonal elements of the corrected stress tensor are all zero and the off-diagonal elements are given by

$$\sigma_{\alpha\beta}\simeq\frac{\tilde{c}k_{\mathrm{B}}T}{4\sqrt{2}}\boldsymbol{\varepsilon}_{\alpha\beta}. \tag{32}$$

Consider the example case of simple shear equivalent to the sliding of two planes, normal to the z axis, $\varepsilon_{yz}=\varepsilon_{zy}=1/2\,\gamma$. The equilibrium shear modulus G is defined as the stress-strain ratio

$$G=\frac{1}{8\sqrt{2}}\tilde{c}k_{\mathrm{B}}T. \tag{33}$$

In the case of a small volume-preserving uniaxial deformation, that is when $\lambda_{zz}=1+\gamma$, we can expand Eq. (30) in terms of the infinitesimal strain γ, and define the Young modulus

$$Y=\frac{3}{8\sqrt{2}}\tilde{c}k_{\mathrm{B}}T. \tag{34}$$

The Young modulus in extension and is three times the shear modulus G, in accordance with the theory of small, homogeneous strains for isotropic incompressible solids.[34] Both constants are, comfortingly, proportional to the classical $\tilde{c}k_{\mathrm{B}}T$, with a hardly relevant numerical factor difference with respect to the phantom chain rubber elasticity.

V. PRACTICAL IMPLICATION II: LINEAR DYNAMIC RESPONSE

The effect of cross-linking during network formation is to transform a viscoelastic liquid (the melt) into a viscoelastic solid (the rubber), the material now acquiring an equilibrium modulus.[35,36] In the transition zone between the glassy state (short times) and the equilibrium rubber plateau the properties of a network are not profoundly different from that of an entangled melt.

Since even basic dynamics of stress relaxation is poorly understood from a theoretical point of view, it is worth applying our first-order constrained Rouse model to a simpler particular case of the generally applicable expression (19). In the remaining sections we specifically consider a small, isovolumetric, uniaxial deformation thus focusing on the linear dynamic-mechanical response functions.

A. Stress tensor after a step strain

Consider a step strain of constant magnitude ε that is applied instantaneously at time $t=0$ to an ideal network sample, that is, $\varepsilon(t)=\varepsilon\,\Theta(t)$. The constitutive equation theory of linear viscoelasticity for a homogeneous deformation relates the strain $E(t)$ and stress $\sigma(t)$ as follows:[35]

$$\sigma_{\alpha\beta}(t)=\int_{-\infty}^{t}Y(t-t')\frac{\partial\varepsilon(t')}{\partial t'}dt', \tag{35}$$

where $Y(t)$ is the dynamic linear-response coefficient, e.g., the Young modulus in the case of uniaxial extension. Thus, for the present case of fixed imposed strain this equation simplifies to a time-dependent version of Hooke's law: $\sigma_{\alpha\beta}(t)=Y(t)\varepsilon$. For a rubbery network $Y(t)$ will relax to a finite value, the equilibrium elastic modulus, defined as $Y_{\mathrm{eq}}=\lim_{t\to\infty}Y(t)$, which has been given in Eq. (34).

Let us apply the model of microscopic stress tensor developed in Sec. III to the case of a step deformation. In order to investigate the entire time spectrum of the linear response, we now need to use the full solution of the Langevin equation (9) describing the normal modes, and depending explicitly on the initial condition,

$$x_{p\alpha}(t)=x_{p\alpha}(0^+)e^{-t/\tau_p}+\frac{1}{\zeta}\int_0^t e^{-(t-t')/\tau_p}\hat{f}_{p\alpha}(t')dt'. \tag{36}$$

Applying the present model embodied by Eq. (19) to this nonequilibrium case is not as straightforward as the equilibrium case has been. The first challenge is to choose an appropriate initial condition $x_{p\alpha}(0)$. From Eq. (9) one finds the

time-correlation functions of the normal modes. In equilibrium, they are given by

$$\langle x_{p\alpha}(t)x_{q\alpha}(0)\rangle_{\psi[f]} = \delta_{pq}\delta_{\alpha\beta}\frac{k_BT}{k_p}e^{-t/\tau_p}, \tag{37}$$

where $\tau_p = \zeta_R/k_p \equiv \tau_R/(p-1/2)^2$ is the relaxation time of the pth Rouse mode, as introduced in Sec. III. In Sec. IV we imposed the constraint that only the topologically quenched cross-links are affected by the deformation, thereby applying the affine deformation approximation only to the span vectors **R**. Here, at arbitrarily short time after an instantaneous strain, we have to assume that the positions of *all* the segments between two cross-links are changed on instantaneous deformation, in the same proportion as the macroscopic strain dictates. Thus, applying a step strain **E** at time $t=0$, a given segment position before deformation $\mathbf{r}_n(0^-)$ will change to $\mathbf{r}_n(0^+)$ after deformation,

$$\mathbf{r}_n(0^+) = \mathbf{E}\cdot\mathbf{r}_n(0^-) \quad \rightarrow \quad \mathbf{x}_p(0^+) = \mathbf{E}\cdot\mathbf{x}_p(0^-). \tag{38}$$

The second equality follows from the fact that the real segment positions $\{\mathbf{r}\}$ are linear functions of the normal coordinates in Eq. (8b). Applying the affine deformation to all normal modes, the right-hand side of Eq. (36) becomes

$$E_{\alpha\mu}x_{p\mu}(0^-)e^{-t/\tau_p} + \frac{1}{\zeta_R}\int_0^t e^{-(t-t')/\tau_p}\hat{f}_{p\alpha}(t')dt'. \tag{39}$$

After substituting this $x_{p\alpha}(t)$ into the main expression for stress in Eq. (19), we obtain an expression with the Gaussian path integrals having quadratic and linear cross terms in the random force f,

$$\begin{aligned}\sigma_{\alpha\beta}(t) = {} & \frac{\tilde{c}}{[\det \mathbf{E}\mathbf{E}^{\mathsf{T}}]^{1/2}}e^{-6/N\ell^2\Sigma_r\Sigma_{\eta,\eta'}E_{\eta\mu'}E_{\eta'\mu'}(\mathbf{E}\mathbf{E}^{\mathsf{T}})^{-1}_{\eta\eta'}(k_BT/k_r)e^{-2t/\tau_r}} \\ & \times\sum_{p=1}^{\infty}k_p\left\{\frac{k_BT}{k_p}E_{\alpha\mu}E_{\beta\mu}e^{-2t/\tau_p}\int[\mathcal{D}f]e^{-1/2\mathbf{f}^{\mathsf{T}}\mathbf{M}\,\mathbf{f}-\mathbf{g}^{\mathsf{T}}\mathbf{f}} + \frac{E_{\alpha\mu}x_{p\mu}(0^-)}{\zeta_R}\int_0^t dx e^{-(2t-x)/\tau_p}\int[\mathcal{D}f]f_{p\alpha}(x)e^{-1/2\mathbf{f}^{\mathsf{T}}\mathbf{M}\,\mathbf{f}-\mathbf{g}^{\mathsf{T}}\mathbf{f}}\right. \\ & \left. + \frac{E_{\beta\nu}x_{p\nu}(0^-)}{\zeta_R}\int_0^t dy e^{-(2t-y)/\tau_p}\int[\mathcal{D}f]f_{p\beta}(y)e^{-1/2\mathbf{f}^{\mathsf{T}}\mathbf{M}\,\mathbf{f}-\mathbf{g}^{\mathsf{T}}\mathbf{f}} + \frac{1}{\zeta_R^2}\int_0^t dx\int_0^t dy\, e^{-(2t-x-y)/\tau_p}\int[\mathcal{D}f]f_{p\alpha}(x)f_{p\beta}(y)e^{-1/2\mathbf{f}^{\mathsf{T}}\mathbf{M}\,\mathbf{f}-\mathbf{g}^{\mathsf{T}}\mathbf{f}}\right\},\end{aligned} \tag{40}$$

where **M** represents the tensor defined in Eq. (22) and the linear term involves a vector **g**, determined by the "memory" of the initial condition, c.f. (39), given by

$$g^q_\eta(t') = \frac{12}{\zeta_R N\ell^2}\sum_r(\mathbf{E}\mathbf{E}^{\mathsf{T}})^{-1}_{\eta,\eta'}E_{\eta'\mu}x_{r\mu}(0^-)e^{-t/\tau_r}e^{-(t-t')/\tau_q}. \tag{41}$$

From Eq. (37), the time-correlation function of the normal modes *before* deformation is equal to $\langle x_{p\alpha}(0^-)x_{q\alpha}(0^-)\rangle = \delta_{pq}\delta_{\alpha\beta}k_BT/k_p$. After performing the functional integrations [see the Appendix, Eq. (A9)] the computation procedure is analogous to the one for the equilibrium case. However, here the calculation involves integrations up to finite time t (instead of $t\rightarrow\infty$ as in Sec. IV), and we are left with these intractable sums:

$$S_1 = \sum_{q=1}^{N}\frac{1}{[q-1/2]^2}, \quad S_2 = \sum_{q=1}^{N}\frac{e^{-2[q-(1/2)]^2t/\tau_R}}{[q-(1/2)]^2}, \qquad S_3 = \sum_{q=1}^{N}e^{-2[q-1/2]^2t/\tau_R}, \quad S_4 = \sum_{q=1}^{N}\frac{e^{-4[q-(1/2)]^2t/\tau_R}}{[q-(1/2)]^2}. \tag{42}$$

Note that all these sums are explicit functions of N and $t/\tau_R(N)$ only (to remind, N is the number of segments on a strand between cross-links). For illustration, a more detailed calculation of a linear term [second term on the 2nd line in Eq. (40)] is explicitly presented in the Appendix [Eq. (A10)]. In the remaining sections we probe the physics of the system without attempting to obtain closed-form solutions for Eq. (42).

B. Uniaxial extension and compressibility

For a uniaxial deformation given by Eq. (24), before accounting for volume relaxation, the nonzero diagonal components of the stress tensor are given by

$$\begin{aligned}\sigma_{\alpha\alpha} = {} & \tilde{c}k_BT\prod_i\frac{1}{\lambda_i}\left[1+\frac{2}{\pi^2}\frac{(S_1-S_2)}{\lambda_i^2}\right]^{-1/2}\exp\left\{\frac{2}{\pi^4}(S_1-S_2)S_2\sum_i\lambda_i^{-2}\left[1+\frac{2}{\pi^2}\frac{(S_1-S_2)}{\lambda_i^2}\right]^{-1}-\frac{3}{\pi^2}S_2\right\} \\ & \times\left\{\lambda_\alpha^2S_3+\left[1+\frac{2}{\pi^2}\frac{(S_1-S_2)}{\lambda_\alpha^2}\right]^{-1}\left(\frac{4(S_2-S_4)}{\pi^2}+\frac{(S_4-2S_2+S_1)}{(S_1-S_2)}\left(1+\frac{4}{\pi^4}(S_1-S_2)S_2\sum_i\lambda_i^{-2}\left[1+\frac{2}{\pi^2}\frac{(S_1-S_2)}{\lambda_i^2}\right]^{-1}\right)\right)\right\}.\end{aligned} \tag{43}$$

The same procedure, as in Sec. IV B, for dealing with volume relaxation after network formation and after imposed strain is applied to the numerical problem, Eq. (43). The first correction, due to the initial volume change on network formation, is of course independent on the subsequent dynamics. The syneresis factor a_0^* is still given by the Eq. (28). The second volume-relaxation factor a^* is time dependent. If we expand it in terms of a small parameter, $1/\tilde{K}$, the inverse of the bulk modulus, its approximate form would illustrate the evolution,

$$a^*(t) = \frac{\tilde{c}k_B T\varepsilon}{3\tilde{K}}\mathfrak{S}[S_1(t),\ldots,S_4(t)] + \mathcal{O}(\tilde{K}^{-2}). \tag{44}$$

Time dependence enters through $\mathfrak{S}$, which is a function of the sums in Eq. (42), and which is explicitly given in the Appendix, Eq. (A11). After inserting a_0^* and $a^*(t)$ into the stress expression Eq. (43) [where for the uniaxial extension the Cartesian factor $\lambda_{zz} \to (1+\varepsilon)(1+a^*)(1+a_0^*)$], one can finally take the $\tilde{K} \to \infty$ limit. The resulting expression gives the relevant stress, adjusted after volume relaxation, which is proportional to the Young modulus, $Y(t) \equiv \sigma(t)/\varepsilon$, or explicitly in terms of the sums:

$$Y(t) = 3\tilde{c}k_B T\,\mathfrak{S}(t). \tag{45}$$

Next, we consider the Poisson ratio n, which is the ratio of transverse contraction strain to longitudinal extension strain in the direction of the stretching force. In a viscoelastic material the Poisson ratio is time dependent for transient tests such as stress relaxation. In other words, the polymeric material is "a lot less incompressible" at very short times after an instantaneous strain is applied. For the current geometry $n(t) = (a(t) - \varepsilon/2)/(a(t) + \varepsilon)$. Written as the dominant term in a $1/\tilde{K}$ expansion, this Poisson ratio takes the simple form

$$n(t) = \frac{1}{2} - \frac{\tilde{c}k_B T}{2\tilde{K}}\mathfrak{S}(t). \tag{46}$$

In isotropic elasticity the Poisson ratio is bounded, $-1 \leqslant n \leqslant 1/2$ and related to the ratio of elastic moduli $\tilde{K}$, Y and the shear modulus G.[34] Comparing Eq. (46) with Eq. (45), we indeed find $n = 1/2 - Y(t)/6\tilde{K}$ independently of time, in accordance with the fundamentals of elasticity. Lastly, we can directly obtain the linear shear modulus $G(t)$ from this analysis, instead of applying a different, simple-shear deformation. This is because an alternative form of the Poisson ratio expansion is $n = 1/2 - G/2\tilde{K}$, and so $G(t) = Y(t)/3 = \tilde{c}k_B T\mathfrak{S}(t)$. In Fig. 3 we show graphically the numerical result of our investigation, with the sums in Eq. (42) evaluated over a broad time range. The left y axis gives the log-log plot of the scaled dynamic shear modulus $G(t)/ck_B T$ versus the scaled time t/τ^* for three different network strand lengths N. The time is reduced by the shortest of all Rouse relaxation times, $\tau^* \equiv \tau_{p=N} = \zeta\ell^2/(3\pi^2 k_B T)$, corresponding to the rate of motion of a single chain segment. Accordingly, the short-time dynamic glass plateau is reached at $t < \tau^*$. The second observation (expected within the realm of Rouse dynamics) is that the slope of the dynamic glass transition very closely follows

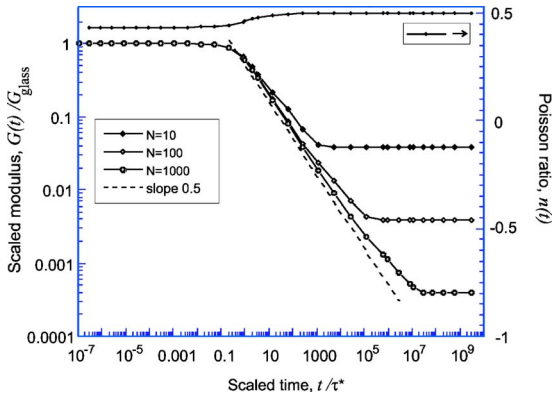

FIG. 3. Linear dynamic-mechanical response within the constrained Rouse model, against dimensionless time t/τ^*, for different cross-link densities, after a small step strain. The left (logarithmic) y axis gives the relaxation of shear modulus, scaled by its universal value in the glass ($t \to 0$) state, $G(t)/ck_B T$. Three sets of data for different N show the different levels of rubber plateau but the slope of the dynamic glass transition nearly following $t^{-0.5}$ law, traced by the dashed line. The right (linear) y axis gives the t evolution of the Poisson ratio n against the same time scale, for $\tilde{K} = 10^9$ Pa, and $\tilde{c} = 1.25 \times 10^{26}$ m^{-3}. The dependence on N is hardly visible in $n(t)$, which reaches the incompressible value $n \approx 0.5$ as soon as $G(t)$ drops below a sufficiently low value.

the $G(t) \propto t^{-0.5}$ law. The log-log slope indicated by the dashed line makes this comparison in the plot. In this transition zone the chain segments try to move to more favorable configuration positions such that the stored elastic energy (from deformation) is reduced. The Rouse relaxation process starts with the high p modes and ends when the last $p = 1$ mode has relaxed. This is expected to happen at $t \sim \tau_R$, after which the equilibrium rubber plateau should set in. Both the Rouse time τ_R and the equilibrium rubber value of $G = \tilde{c}k_B T/8\sqrt{2}$ are functions of N, as clearly seen in the graphs. In contrast, the glassy modulus in this model G_{glass} is universal, being proportional to $\tilde{c}Nk_B T$, that is, the total monomer (segment) density c.

The other set of data in Fig. 3 is a plot of the Poisson's ratio n, also against t/τ^*. In this case we plot a full numerical expression, not the expansion in $1/\tilde{K}$ as discussed earlier. The graph clearly indicates the transition from a Poisson ratio significantly lower than 0.5, eventually reaching the "incompressible" value as $t/\tau^* \gg 1$. Interestingly, this transition does not depend on N (or, in other words, network cross-link density), at least for large N. Since $n(t)$ is always determined by the ratios of shear and bulk moduli, $G/\tilde{K}$, its reduction to $n = 0.5$ occurs when $G(t)$ diminishes to a value significantly lower than $\tilde{K}$. This takes place somewhere along the $\sim t^{-0.5}$ relaxation, in most cases well before the rubber-plateau onset.

C. Stress tensor: Limiting cases

The sums in Eq. (42) depend on the value of the time t at which the stress is measured and are explicit functions of N and $t/\tau_R(N)$ only. In the short-time limit, $t \to 0$, we obtain straightforwardly

$$\sigma_{\alpha\beta} = \frac{\tilde{c}}{[\mathrm{Det}\,\mathbf{E}\mathbf{E}^{\mathsf{T}}]^{1/2}} \sum_{p=1}^{\infty} k_p E_{\alpha\mu} E_{\beta\nu} \langle x_{p\mu}(0^-) x_{p\nu}(0^-) \rangle$$
$$= \tilde{c} k_{\mathrm{B}} T\, N [\mathrm{Det}\,\mathbf{E}\mathbf{E}^{\mathsf{T}}]^{-1/2} (\mathbf{E}\mathbf{E}^{\mathsf{T}})_{\alpha\beta}. \quad (47)$$

At short times a large force is generated in response to the instantaneous step strain and this is expected to affect the network chains on the local monomer (segment) length scale. Equation (47) gives the stress in the glass regime, before accounting for volume relaxation, as discussed in Sec. V B. Substituting the small uniaxial extension and performing the volume adjustment operation, we directly obtain the Young's modulus on the glassy plateau, $Y_{\mathrm{glass}} = 3\tilde{c}N\, k_{\mathrm{B}}T \equiv 3c\, k_{\mathrm{B}}T$, and the shear modulus $G_{\mathrm{glass}} = Y/2(1+n)$. Deviations of G_{glass} from $3Y$ and of the Poisson's ratio from 0.5 are, as usual, of the order $Y_{\mathrm{glass}}/\tilde{K}$. This factor, however, does not have to be small. In the present theory the glass moduli are appropriately large (factor of N higher than the rubber moduli), but of course this misses much of the specifics of glass phase and there could be factors making these moduli even higher in reality (e.g., not simply proportional to $k_{\mathrm{B}}T$).

In the long-time limit, i.e., $t \to \infty$, the stress tensor simplifies the previous equilibrium case result of Eq. (23) giving the rubber-plateau shear modulus $G_{\mathrm{eq}} = \tilde{c} k_{\mathrm{B}} T/8\sqrt{2}$. If we consider the approach towards this equilibrium, at $t > \tau_R$, the sums in Eq. (42) are dominated by the first term ($q=1$) and we may approximate them by these leading terms. For example, $S_1 \simeq \pi^2/2$ and $S_2 \simeq 4e^{-t/2\tau_R}$. The final, nonzero stress of a system subjected to a small, isovolumetric uniaxial deformation $\lambda = 1+\varepsilon$, at times $t > \tau_R$, after taking account of the usual two-step syneresis, is then

$$\sigma_{zz}(t) \approx \frac{3\tilde{c} k_{\mathrm{B}} T}{2\sqrt{2}} \left[1 + 4\left(1 - \frac{3}{\pi^2}\right) e^{-t/2\tau_R} \right] \varepsilon, \quad (48)$$

which shows the last remnant of relaxation of the longest ($p=1$) Rouse mode for an average chain. Note that the relaxation modulus $G(t)$ depends implicitly on N in various ways. Firstly, through the cross-link density $\tilde{c} = c/N$, but also via the Rouse time $\tau_R \propto N^2$. The role of the factor N can be seen in Fig. 3, the equilibrium rubber plateau is reached sooner as N decreases (increasing cross-link density).

VI. CONCLUSIONS

We have developed a simple model for the purpose of investigating the linear dynamic response of a polymer network, based on the naturally dynamic Rouse model and incorporating various constraints arising in the polymer network. The model predictions can be summarized as follows. Firstly, for long times ($t > \tau_R$) we obtain a constant rubber-elastic plateau (with associated Poisson ratio of $\frac{1}{2}$), which depends on temperature and the average cross-link density of the network. At short times we found a constant high-level plateau, a few orders of magnitude (N) larger than the equilibrium modulus value, which we associate with and call the glassy plateau. As expected, we obtained a Rouse-power law $\sim t^{-1/2}$ for time scales when the large number of Rouse modes is still relaxing.

Section III captured the essence of the dynamic stress-tensor approach, and laid the groundwork before attempting the real dynamic-mechanical problem in Sec. V C. The quenched permanent cross-linking was treated in a similar way to elementary phantom models—by averaging the deformed span vectors over the initial distribution function of the undeformed end-to-end vector between links, and asserting that these deformed span vectors deform affinely. For the dynamical case, especially allowing for short times, Sec. V, this assumption was modified by allowing *each* monomer (or chain segment) to deform affinely assuming that in the $t \to 0$ (glass) limit the system is completely frozen. This introduced the "memory" of the initial condition into the Langevin stochastic problem and generated the plausible macroscopic dynamics. Whether this is an acceptable treatment remains open to question.

Many improvements in this model are possible and required. Firstly, there is the question of working with a more physically appropriate, initial condition: how does one describe the monomer motion and chain configuration immediately after a step strain is applied? In this work, we essentially used equilibrium pair-correlation functions $\langle x_{p\alpha} x_{q\alpha} \rangle$ to describe nonequilibrium phenomena. It is expected that the Rouse model breaks down at short times (or at high frequencies) when the segment-segment bonds, taken as harmonic here, are modified by the sudden imposed force. In future we shall have to employ theoretical apparatus for studying glassy dynamics to enable a more precise examination of polymer network dynamic response and treat the "upper plateau" of $G(t)$ in a better way, accounting for additional forces at $t \to 0$.

In all of the calculations, we assumed a phantom model. Thus, an obvious improvement of the model would be to include trapped entanglements and excluded volume effects. This extension could, for example, be based on a tube or slip-link model with nonaffine deformation.[3] Accounting for the nonlocal multichain correlations between the dynamics of randomly linked strands should generally improve the long-time description of the "lower plateau" of $G(t)$.

Lastly, in this model we have assumed the cross-links to be spatially fixed and to deform affinely. Experiments have shown that network deformations at a microscopic length scale are not affine.[20,37] Future improvements of this work will attempt to constrain the cross-links less rigidly. Talking about experimental observations on rubber relaxation, in detailed literature one finds that neither glassy nor rubber plateau has a constant slope. In equilibrium the rubbery network may take days to fully relax, following very slow functions ($t^{-0.1}$, if not logarithmic). This reflects more complex effects of multichain correlations, dangling ends, and entanglements. The glassy plateau also has a time dependence, a few decades higher than the present prediction, due to continuing relaxation of intrasegmental motion modes (often referred to as β relaxation, etc.) Further, for networks consisting of real chains the dynamic glass transition slope is often in the range

of $-\frac{2}{3}$ rather than our -0.5. This is similar to a Zimm-model value, although it is hard to find a physical reason to include hydrodynamic effects in a dense solvent-free rubber network. Many mysteries remain untouched in this old field.

ACKNOWLEDGMENTS

Financial assistance of Gonville and Caius College and the Commonwealth Fellowship Plan is hereby acknowledged. We are grateful for many discussions with Sir Sam Edwards, Peter Olmsted, and Mark Warner.

APPENDIX: MATRIX MANIPULATION

For fixed coordinate components $\{\gamma,\nu\}$, the Rouse mode indices $\{q,r\}$ and fixed time positions $\{t',t''\}\leqslant t$, the tensor $\mathbf{M}$ defined in Eq. (22) is explicitly given by

$$\mathbf{M}_{qr}^{\gamma\nu}(t',t'') = (2\zeta_R k_B T)^{-1}\mathbf{I} + b_{qr}^{\gamma\nu} e^{-(t-t')/\tau_q} e^{-(t-t'')/\tau_r} \equiv A\mathbf{I} + b\mathbf{B}. \tag{A1}$$

The shape of this matrix in the $\{t',t''\}$ space is

$$\begin{array}{c} \\ -\infty \\ \vdots \\ \vdots \\ \vdots \\ t''=t \\ \downarrow \\ \infty \end{array} \overset{\begin{array}{c} -\infty \cdots\cdots\cdots t'=t\to\infty \end{array}}{\left(\begin{array}{cccccc} A & \tilde{b}_{qr}^{\gamma\nu}e^{-T_1/\tau_q-T_2/\tau_r} & \cdots & \tilde{b}_{qr}^{\gamma\nu}e^{-T_1/\tau_q} & & \\ \tilde{b}_{qr}^{\gamma\nu}e^{-T_2/r_q-T_1/\tau_r} & A+\tilde{b}_{qr}^{\gamma\nu}e^{-T_2/\tau_q-T_2/\tau_r} & \cdots & \tilde{b}_{qr}^{\gamma\nu}e^{-T_2/\tau_q} & & \\ \tilde{b}_{qr}^{\gamma\nu}e^{-T_3/\tau_q-T_1/\tau_r} & \tilde{b}_{qr}^{\gamma\nu}e^{-T_3/\tau_q-T_2/\tau_r} & A+\tilde{b}_{qr}^{\gamma\nu}e^{-T_3/\tau_q-T_3/\tau_r} & & \vdots & 0 \\ \vdots & \vdots & \vdots & \vdots & & \\ \tilde{b}_{qr}^{\gamma\nu}e^{-T_1/\tau_r} & \tilde{b}_{qr}^{\gamma\nu}e^{-T_2/\tau_r} & \cdots & A+\tilde{b}_{qr}^{\gamma\nu} & & \\ & & & & A & \\ & 0 & & & & A \\ & & & & & \ddots \end{array}\right)}, \tag{A2}$$

where and $T_1\equiv(t-t_1)$, etc. Here we have temporarily discretized time for the sake of illuminating the properties of this matrix. The functional Gaussian integral [given by the second line in Eq. (21)] evaluates to

$$\mathbb{I} \equiv \frac{\int [\mathcal{D}f] f_{p\alpha}(x) f_{p\beta}(y) \exp\left\{ -\frac{1}{2}\sum_{\gamma,\nu=1}^{3}\sum_{q,r}\int dt' \int dt'' f_{q\gamma}(t')\mathbf{M}_{qr}^{\gamma\nu}(t',t'')f_{r\nu}(t'')\right\}}{\int [\mathcal{D}f]\exp\left\{-(4\zeta_R k_B T)^{-1}\sum_{\gamma,\nu=1}^{3}\sum_{q,r}\int dt' \int dt'' f_{q\gamma}(t')\delta_{\gamma\nu}\delta_{qr}\delta(t'-t'')f_{r\nu}(t'')\right\}} = \mathfrak{N}\frac{(2\pi)^{3/2}(\mathbf{M}^{-1})_{pp}^{\alpha\beta}(x,y)}{[\mathrm{Det}\,\mathbf{M}]^{1/2}}, \tag{A3}$$

where x and y are the time arguments of the stochastic force, the second moment of which we are evaluating, cf. Eq. (21). The normalization factor $\mathfrak{N}=(2\pi)^{-3/2}\exp(\frac{1}{2}\mathrm{Tr}\ln A\mathbf{I})$ is defined as the denominator in the first big fraction in Eq. (A3). In order to calculate the determinant we use the identity, $\ln(\mathrm{Det}\,\mathbf{M})^{1/2}=\frac{1}{2}[\mathrm{Tr}\ln A\mathbf{I}+\mathrm{Tr}\ln(\mathbf{I}+b\,\mathbf{B}/A)]$, and the series representation of the logarithm:

$$\frac{1}{2}\mathrm{Tr}\ln\left(\mathbf{I}+\frac{b}{A}\mathbf{B}\right) = \frac{1}{2}\mathrm{Tr}\sum_{n=1}^{\infty}\frac{(-1)^{n+1}}{n}\left(\frac{b}{A}\right)^n\mathbf{B}^n = \frac{1}{2}\sum_{n=1}^{\infty}\frac{(-1)^{n+1}}{n}\left(\frac{b}{A}\right)^n\mathrm{Tr}\{[B_{t',t'';q,r}^{\gamma\nu}]^n\},$$

where the trace accounts for the summation over all relevant indices in the matrix $\mathbf{B}$

$$\mathrm{Tr}\{[\ ]\} = \mathrm{Tr}\left\{\left[\sum_{j_1\cdots j_{n-1}=1}^{d_t}\sum_{l_1\cdots l_{n-1}=1}^{d_q}\sum_{k_1\cdots k_{n-1}=1}^{3} B_{t',j_1;q,l_1}^{\gamma k_1}B_{j_1,j_2;l_1,l_2}^{k_1,k_2}\cdots B_{j_{n-1},t'';l_{n-1},r}^{k_{n-1}\nu}\right]\right\} \tag{A4}$$

$$= \mathrm{Tr}\left\{\sum_{\{j_i\};\{l_i\};\{k_i\}}(-1)^{q+l_1}(\mathbf{E}\mathbf{E}^{\mathsf{T}})_{\gamma k_1}^{-1}e^{-(t-t')/\tau_q-(t-j_1)/\tau_{l_1}}\cdots(-1)^{l_{n-1}+r}(\mathbf{E}\mathbf{E}^{\mathsf{T}})_{k_{n-1}\nu}^{-1}e^{-(t-j_{n-1})/\tau_{l_{n-1}}-(t-t'')/\tau_r}\right\}$$

$$= \mathrm{Tr}\{(\mathbf{E}\mathbf{E}^{\mathsf{T}})^{-n}\}\left(\sum_{q=1}^{q_{\max}}\int_{-\infty}^{t}dt' e^{-2(t-t')/\tau_q}\right)^n = \mathrm{Tr}\{(\mathbf{E}\mathbf{E}^{\mathsf{T}})^{-n}\}\left(\sum_{q=1}^{\infty}\frac{\tau_q}{2}\right)^n, \tag{A5}$$

where the mode relaxation times are given, to remind the reader, by $\tau_q = \zeta N^2 \ell^2/(3\pi^2 k_B T q^2)$. Since $b/A\Sigma_q \tau_q/2 \equiv 1$, by construction, the most general expression for the determinant is given by

$$(\mathrm{Det}\,\mathbf{M})^{1/2} = \exp\left(\frac{1}{2}\mathrm{Tr}\ln A\mathbf{I} + \frac{1}{2}\sum_n \frac{(-1)^{n+1}}{n}\mathrm{Tr}\{(\mathbf{E}\mathbf{E}^{\mathsf{T}})^{-n}\}\right). \tag{A6}$$

Similarly, to compute the second moment of the stochastic force $\mathbf{f}_p(t)$ via the Gaussian integral, we need to calculate the following inverse matrix element:

$$(\mathbf{M}^{-1})^{\alpha\beta}_{pp}(x,y) = [(A\mathbf{I} + b\mathbf{B})^{-1}]^{\alpha\beta}_{pp,xy} = \frac{1}{A}\sum_{n=0}^{\infty}(-1)^n\left(\frac{b}{A}\right)^n [B^{\alpha\beta}_{x,y;p,p}]^n. \tag{A7}$$

At this point we write the product of n terms in an expanded form in order to observe the necessary cancellations in the exponents, as in Eq. (A4), but without taking the final trace.

$$(\mathbf{M}^{-1})^{\alpha\beta}_{pp}(x,y) = \frac{1}{A}\sum_{n=0}^{\infty}(-1)^n \times\left[\sum_{\{j_i\};\{l_i\};\{k_i\}} B^{\alpha k_1}_{x,j_1;p,l_1}\cdots B^{k_{n-1}\beta}_{j_{n-1},y;l_{n-1},p}\right] = \frac{48(k_B T)^2}{N\ell^2}e^{-(2t-x-y)/\tau_p}[\delta_{\alpha\beta} + (\mathbf{E}\mathbf{E}^{\mathsf{T}})^{-1}_{\alpha\beta}]^{-1}. \tag{A8}$$

These equations are combined to produce the final form of the equilibrium stress tensor before volume relaxation, Eq. (23), as well as in the computation of the dynamic response. In the linear-response case (Sec. V), the full solution of $x_{p\alpha}(t)$ given by Eq. (39) leads to the linear terms in the stochastic force $\mathbf{f}_p(t)$ and the three different Gaussian functional integrals are solved,

$$\int [\mathcal{D}f] e^{-1/2\mathbf{f}^{\mathsf{T}}\mathbf{M}\,\mathbf{f} - \mathbf{g}^{\mathsf{T}}\mathbf{f}} = \mathfrak{N}(2\pi)^{3/2}[\mathrm{Det}\,\mathbf{M}]^{-1/2} e^{1/2\mathbf{g}^{\mathsf{T}}\mathbf{M}^{-1}\mathbf{g}}, \tag{A9a}$$

$$\int [\mathcal{D}f] f_{p\alpha}(x) e^{-1/2\mathbf{f}^{\mathsf{T}}\mathbf{M}\,\mathbf{f} - \mathbf{g}^{\mathsf{T}}\mathbf{f}} = \mathfrak{N}(2\pi)^{3/2}\left(-\sum_r \int_0^t dt' (\mathbf{M}^{-1})^{pr}_{\alpha\nu}(x,t') g^r_\nu(t')\right) \times [\mathrm{Det}\,\mathbf{M}]^{-1/2} e^{1/2\mathbf{g}^{\mathsf{T}}\mathbf{M}^{-1}\mathbf{g}}, \tag{A9b}$$

$$\int [\mathcal{D}f] f_{p\alpha}(x) f_{p\beta}(y) e^{-1/2\mathbf{f}^{\mathsf{T}}\mathbf{M}\,\mathbf{f} - \mathbf{g}^{\mathsf{T}}\mathbf{f}} = \mathfrak{N}(2\pi)^{3/2}(\mathbf{M}^{-1})^{pp}_{\alpha\beta,xy}(\mathbf{I} + \mathbf{g}^{\mathsf{T}}\mathbf{M}^{-1}\mathbf{g}) \times [\mathrm{Det}\,\mathbf{M}]^{-1/2} e^{1/2\mathbf{g}^{\mathsf{T}}\mathbf{M}^{-1}\mathbf{g}}. \tag{A9c}$$

Recall the normalization factor $\mathfrak{N}$ first introduced in Eq. (A3), as well as the tensor $\mathbf{M}$ of Eq. (A1) and the additional vector $\mathbf{g}$ given by Eq. (41). The linear term in the stress tensor in Eq. (40) for the dynamical case, after the functional integrals are evaluated, is shown below to illustrate the origin of the time-dependent sums $S_1 - S_4$:

$$-\frac{24k_B T}{\zeta_R N\ell^2}E_{\alpha\mu}x_{p\mu}(0^-)\int_0^t dx e^{-(3t-2x)/\tau_p}\sum_\nu\left[1 + \frac{2}{\pi^2}(EE^{\mathsf{T}})^{-1}_{\alpha\nu}\sum_q \frac{1}{[q-(1/2)]^2}(1 - e^{-2t/\tau_q})\right]^{-1}\sum_{r'} E^{\mathsf{T}-1}_{\nu\mu'}x_{r'\mu'}(0^-)e^{-t/\tau_{r'}} \times \exp\left(\frac{2}{\pi^4}\sum_q \frac{1}{[q-(1/2)]^2}(1 - e^{-2t/\tau_q})\sum_r \frac{1}{[r-(1/2)]^2}e^{-2t/\tau_r}\sum_{\eta,\eta'} E^{\mathsf{T}-1}_{\eta\mu'}E^{\mathsf{T}-1}_{\eta'\mu'}\left[1 + \frac{2}{\pi^2}(EE^{\mathsf{T}})^{-1}_{\eta\eta'}\sum_q \frac{1}{[q-(1/2)]^2}(1 - e^{-2t/\tau_q})\right]^{-1}\right) \times \exp\left(-\frac{1}{2}\sum_n \frac{(-1)^{n+1}}{n}\mathrm{Tr}\{(\mathbf{E}\mathbf{E}^{\mathsf{T}})^{-n}\}\left[\frac{2}{\pi^2}\sum_q \frac{1}{[q-(1/2)]^2}(1 - e^{-2t/\tau_q})\right]^n\right). \tag{A10}$$

Lastly (not shown here), the combination of initial-condition normal coordinates is replaced by its equilibrium value before deformation, $x_{p\mu}(0^-)x_{r'\mu'}(0^-) \to \delta_{pr'}\delta_{\mu\mu'}k_B T/k_p$. This allows us to explicitly perform the sum over p and the integration with respect to x. Here the deformation $\mathbf{E}$ is fully arbitrary and we sum over repeated Cartesian indices (e.g., μ').

Finally, the second syneresis factor in Eq. (44), Poisson's ratio in Eq. (46), Young's modulus, and dynamic modulus all depend on the following function of time, whose long expression is nevertheless explicit (the sums $S_1 - S_4$ are defined by Eq. (42) in the main text):

$$\begin{aligned}\mathfrak{S}(t) = \pi^3[&\pi^6 S_3 + 2\pi^4(3(S_1 - S_2)S_3 + S_4 + S_1 - 2S_2) \\ &+ 4\pi^2(S_1 - S_2)(3(S_1 - S_2)S_3 + 3S_4 + S_1 - 4S_2) \\ &+ 8(S_1 - S_2)((S_1 - S_2)^2 S_3 - 2(S_1 - S_2)(S_2 - S_4) \\ &+ 3S_2(S_4 + S_1 - 2S_2))]e^{-3S_2/[\pi^2 + 2(S_1 - S_2)]} \\ &\times[\pi^2 + 2(S_1 - S_2)]^{-9/2}.\end{aligned} \tag{A11}$$

[1] W. Kuhn, Kolloid-Z. **68**, 2 (1934).
[2] R. C. Ball, S. F. Edwards, M. Doi, and M. Warner, Polymer **22**, 1010 (1981).
[3] S. F. Edwards and T. A. Vilgis, Rep. Prog. Phys. **51**, 243 (1988).
[4] B. Mergell and R. Everaers, Macromolecules **34**, 5675 (2001).
[5] S. F. Edwards and M. Doi, *The Theory of Polymer Dynamics* (Clarendon, Oxford, 1986).
[6] D. W. Mead, R. G. Larson, and M. Doi, Macromolecules **31**, 7895 (1998).
[7] R. S. Graham, A. E. Likhtman, T. C. B. McLeish, and S. T. Milner, J. Rheol. **47**, 1171 (2003).
[8] H. Watanabe, Prog. Polym. Sci. **24**, 1253 (1999).
[9] A. D. Roberts, *Natural Rubber Science and Technology* (Clarendon, Oxford, 1988).
[10] S. F. Edwards, Proc. Phys. Soc. London **92**, 513 (1967).
[11] P. G. De Gennes, J. Chem. Phys. **55**, 572 (1971).
[12] S. F. Edwards and M. Doi, J. Chem. Soc., Faraday Trans. 2 **74**, 1789 (1978).
[13] P. J. Flory, *Statistical Mechanics of Chain Molecules* (Interscience, New York, 1969).
[14] S. F. Edwards, J. Phys. A **7**, 318 (1974).
[15] S. Edwards, H. Takano, and E. M. Terentjev, J. Chem. Phys. **113**, 5531 (2000).
[16] H. M. James and E. Guth, J. Chem. Phys. **11**, 455 (1943).
[17] S. Panyukov and Y. Rabin, Phys. Rep. **269**, 1 (1996).
[18] R. T. Deam and S. F. Edwards, Philos. Trans. R. Soc. London, Ser. A **280**, 317 (1976).
[19] P. G. De Gennes, *Scaling Concepts in Polymer Physics* (Cornell University Press, Ithaca, 1985).
[20] J. Bastide and L. Leibler, Macromolecules **21**, 2647 (1988).
[21] E. S. Matsuo, M. Orkisz, S. Sun, Y. Li, and T. Tanaka, Macromolecules **27**, 6791 (1994).
[22] P. Goldbart and N. Goldenfeld, Phys. Rev. A **39**, 1402 (1989).
[23] P. Goldbart and N. Goldenfeld, Phys. Rev. A **39**, 1412 (1989).
[24] M. Mooney, J. Polym. Sci. **304**, 599 (1959).
[25] Y. Marciano and F. Brochard-Wyart, Macromolecules **28**, 985 (1995).
[26] S. Quake, H. Babcock, and S. Chu, Nature (London) **388**, 151 (1997).
[27] H. Tang, Macromolecules **29**, 2633 (1996).
[28] L. R. G. Treloar, *The Physics of Rubber Elasticity* (Clarendon, Oxford, 1975).
[29] M. Warner and E. M. Terentjev, *Liquid Crystal Elastomers* (Oxford University Press, Oxford, 2003).
[30] S. S. Antman and R. S. Marlow, Atti Accad. Naz. Lincei, Cl. Sci. Fis., Mat. Nat., Rend. **70**, 256 (1982).
[31] S. S. Antman and R. S. Marlow, Arch. Ration. Mech. Anal. **116**, 257 (1991).
[32] M. Gottlieb and R. Gaylord, Polymer **24**, 1644 (1983).
[33] R. J. Young and P. A. Lovell, *Introduction to Polymers*, 2nd ed. (Stanley Thornes, Cheltenham, Great Britain, 1991).
[34] L. D. Landau and E. M. Lifshitz, *Theory of Elasticity* (Pergamon, Oxford, 1986).
[35] J. D. Ferry, *Viscoelastic Properties of Polymers* (Wiley, New York, 1980).
[36] J. D. Ferry, L. D. Grandine, and E. R. Fitzgerald, J. Appl. Phys. **24**, 911 (1953).
[37] S. Westermann, W. Pyckout-Hintzen, D. Richter *et al.*, Macromolecules **34**, 2186 (2001).